ANALYSIS OF POTENTIAL FLOW AROUND TWO-DIMENSIONAL HYDROFOIL BY SOURCE BASED LOWER AND HIGHER ORDER PANEL METHODS

(Date received: 21.5.2008)

Md. Shahjada Tarafder[1], Gazi Md. Khalil[2] and Muhammad Rabiul Islam[3]
[1,2,3]Department of Naval Architecture and Marine Engineering
Bangladesh University of Engineering and Technology
Dhaka-1000, Bangladesh
E-mail: shahjada68@yahoo.com.[1]

ABSTRACT

This paper deals with the computation of potential flow problem around the two-dimensional hydrofoil without considering the effect of free surface by the source based lower and higher order panel methods. Using Green's second identity the Laplace equation is transformed into an integral equation in terms of a distribution of singular solutions, such as sources on the boundaries. After satisfying the boundary conditions the integral equation can be written into a matrix form and the matrix is solved by Gaussian Elimination procedure. The validity of the computer scheme is examined by comparing the numerical results with the analytical as well as experimental results of van de Vooren and NACA 0012 hydrofoils. In comparison to the higher order method, the use of the lower order method results in fewer numerical manipulations and hence less computational time. Each method has the problem near the trailing edge of the hydrofoil.

Keywords: *Kutta Condition, Lower and Higher Order Panel Method, Potential Flow, NACA 0012 Hydrofoils and van de Vooren*

1.0 INTRODUCTION

Hydrofoil is a winglike structure attached to the hull of a boat that raises all or part of the hull out of the water when the boat is moving forward, reducing drag. The practical importance of hydrodynamic analysis of hydrofoils moving under a free surface is very well-known. Thin-foil approximation and the Neumann boundary condition were generally used. Giesing and Smith [1] distributed the Kelvin wave source on the hydrofoil surface, which satisfies the linearised free surface condition, and they obtained an integral equation for the source strength by applying the kinematic Neumann body boundary condition. This integral equation was solved numerically.

Hough and Moran [2] studied thin-foil approximation with linearised free surface condition. They examined the flow around flat-plate and cambered-arc hydrofoils. Salvesen and Von Kerczek [3,4] first computed steady nonlinear free-surface waves due to a two-dimensional hydrofoil and a point vortex under the free surface by a finite-difference iterative technique. Bai [5] applied the localised finite element numerical technique using Galerkin's method. In this method, an integral equation on the hydrofoil surface is replaced by a system of equations, over a much larger fluid domain but having a much simpler kernel. Yeung and Bouger [6] used a hybrid integral equation method based on Green's theorem. They satisfied the linearised free surface condition and the exact body boundary condition.

Kennell and Plotkin [7] addressed the potential flow about a thin two-dimensional hydrofoil moving with constant velocity at a fixed depth beneath a free surface. The thickness-to-chord ratio of the hydrofoil and disturbances to the free stream were assumed to be small. These small perturbation assumptions were used to produce first-and second-order sub problems structured to provide consistent approximations to boundary conditions on the body and the free surface.

Forbes [8] presented a method for computing two-dimensional potential flow about a wing with a cusped trailing edge immersed beneath the free surface of a running stream of infinite depth. The full non-linear boundary conditions were retained at the free surface of the fluid and the conditions on the hydrofoil were also stated exactly. The problem was solved numerically using integral-equation technique combined with Newton's method. Bai and Han [9] applied the localised finite element method to solve the nonlinear problem. Wu and Eatock Taylor [10] compared the finite element method with the boundary element method for the nonlinear time stepping solution of 2-D hydrofoils.

Bal [11] described a potential-based panel method for the hydrodynamic analysis of 2-D hydrofoils moving under a free surface with constant speed without consideration of the cavitation phenomenon. By applying Green's theorem and choosing the value of internal potential as equal to the incoming flow potential, an integral equation for the total potential was obtained under the potential flow theory. The free surface condition was linearised and the Dirichlet boundary condition was used instead of the Neumann boundary condition. The 2-D hydrofoil was approximated by line panels on which there were only constant doublet distributions. The method of image was used for satisfying the linearised free surface condition and all the terms in the fundamental solution of total potential were integrated over a line panel.

Bal [12] addressed steady cavitating flows around swept and *V*-type hydrofoils under a free surface by using an iterative numerical method. The iterative nonlinear numerical method based on Green's theorem allowed separating cavitating hydrofoil problem and free surface problem. These two problems were solved separately with the effect of one on the other being accounted for in an iterative manner. Cavitating hydrofoil surface and the free surface were modeled numerically with constant strength doublet and constant strength source panel. The source strength on the free surface was expressed in terms of perturbation potential by applying the free surface condition. No radiation condition was enforced for the downstream and transverse boundary on the free surface.

Tarafder *et. al*. [13] presented the Rankine source panel for the potential flow around the two-dimensional body moving under a free surface. The method of image is used to satisfy the linearised free surface condition. In addition, an iterative panel method has been applied for surface piercing hydrofoils without cavitation in Hsin and Chou [14]. Kim [15] and Ragab [16] solved the submerged high speed hydrofoil problem without cavitation.

The aim of this paper is to present the basic mathematical theory behind the lower and higher order source based panel methods and draw a comparison in order to find the suitable method for the analysis of the potential flow around the hydrofoils without considering the effect of free surface.

2.0 MATHEMATICAL MODELLING OF THE PROBLEM

Consider a hydrofoil fixed in a stream of uniform flow with a velocity Q_∞ as shown in Figure 1. The depth of water from the mean line of the hydrofoil is h. A Cartesian co-ordinate system is placed on the free surface and the components of the free stream velocity Q_∞ in the x-z frame of reference are U_∞ and W_∞ respectively. The angle of attack α is defined as the angle between the free stream velocity and the x-axis

$$\alpha = tan^{-1} \frac{W_\infty}{U_\infty}$$

It is assumed that the fluid is inviscid, incompressible and the flow irrotational. The perturbation velocity potential ϕ is defined by $\Phi = \phi + \Phi_\infty$

where, $\Phi_\infty = U_\infty x + W_\infty z = x\, Q_\infty \cos\alpha + z\, Q_\infty \sin\alpha$

The total velocity potential Φ_∞ satisfies the Laplace equation

$$\nabla^2\Phi = 0 \qquad (1)$$

in the fluid domain Ω. The domain Ω is bounded by the body surface S_B, wake surface S_W and an outer control surface S_∞ surrounding the body and the wake surface. Now the problem for the hydrofoil can be constructed by specifying the boundary conditions as follows:

(a) The velocity component normal to the solid boundaries of the hydrofoil must be zero and in a frame of reference:

$$\nabla\Phi \,.\, n = 0 \qquad (2)$$

where n is a unit normal vector directed outward from the fluid domain Ω.

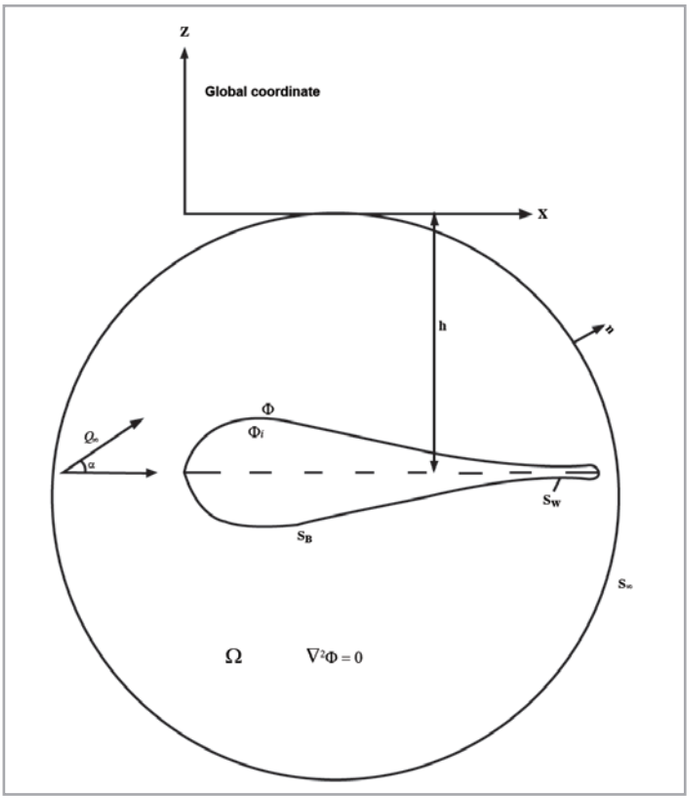

Figure 1 : Potential flows over a closed body

(b) The disturbance induced by the hydrofoil will decay far from the body

$$\lim_{r\to\infty} \nabla\Phi = Q_\infty \qquad (3)$$

which is automatically fulfilled by the singular solutions such as for the source, doublet or the vortex elements.

(c) A proper solution for the doublet distribution will have to fulfil the Kutta condition at the trailing edge of the lifting body such that the potential jump across the wake surface S_W is the same as the circulation and is constant in the streamwise direction on S_W. If the velocity potential inside the body surface S_B is defined by Φ_i then,

$$[\Delta\Phi]_{on\ S_W} = \Phi - \Phi_i = \Gamma = \text{Constant}$$
$$= \Delta\Phi_{T.E.} \qquad (4)$$

3.0 THE GENERAL SOLUTION BASED ON GREEN'S IDENTITY

Applying Green's Second identity the Laplace equation can be transformed into an integral equation as:

$$\Phi(P) = -\frac{1}{2\pi} \int_S (1n\, r\nabla\Phi - \Phi\nabla\, 1n\, r).n\, dS$$

in which the boundary S is composed of S_B, S_W and S_∞. If the point of singularity lies inside the domain Ω, the velocity potential can be expressed as

$$\Phi(P) = -\frac{1}{2\pi} \int_{S_B} (1n\, r\, \nabla(\Phi - \Phi_i) - (\Phi - \Phi_i)\, \nabla\, 1n\, r)\, .\, n\, dS$$

$$+\frac{1}{2\pi}\int_{S_W}\Phi\, n\,.\,\nabla\,1\mathrm{n}\,r\,dS+\Phi_\infty(p) \tag{5}$$

If the difference between the external and internal potentials or the difference between the normal derivative of the external and internal potentials by

$$-\mu=\Phi-\Phi_i \tag{6}$$

$$-\sigma=\frac{\partial\Phi}{\partial\mathrm{n}}-\frac{\partial\Phi_i}{\partial\mathrm{n}} \tag{7}$$

the integral equation (5) can be written as

$$\Phi(P)=\frac{1}{2\pi}\int_{S_B}\left[\sigma\,1\mathrm{n}\,r-\mu\frac{\partial}{\partial n}(1\mathrm{n}\,r)\right]dS$$
$$-\frac{1}{2\pi}\int_{S_W}\left[\mu\frac{\partial}{\partial n}(1\mathrm{n}\,r)\right]dS+\Phi_\infty(P) \tag{8}$$

The elements μ and σ in Equations (6) and (7) are called the strength of the doublet and source respectively and the minus sign is a result of the normal vector n pointing into S_B. To satisfy the Neumann boundary condition of Equation (2) directly, the velocity field due to the singularity distribution of Equation (8): is used

$$\nabla\Phi(x,\,y)=\frac{1}{2\pi}\int_{S_B}\sigma\nabla(1\mathrm{n}\,r)\,dS$$
$$-\frac{1}{2\pi}\int_{S_B+S_W}\mu\nabla\left[\frac{\partial}{\partial\mathrm{n}}(1\mathrm{n}\,r)\right]dS+\nabla\Phi_\infty \tag{9}$$

If the singularity distribution strengths σ and μ are known, then Equation (9) describes the velocity field everywhere (of course special treatment is needed when the velocity is evaluated on the surface S_B). Substitution of Equation (9) into the boundary condition in Equation (2) results in

$$\left\{\frac{1}{2\pi}\int_{S_B}\sigma\nabla(1\mathrm{n}\,r)dS\right.$$
$$\left.-\frac{1}{2\pi}\int_{S_B+S_W}\mu\nabla\left[\frac{\partial}{\partial\mathrm{n}}(1\mathrm{n}\,r)\right]dS+\nabla\Phi_\infty\right\}.n=0 \tag{10}$$

This equation is the basis for many numerical solutions and should hold for every point on the surface S_B. To construct a numerical solution the surface S is divided into N panels and the integration is performed for each panel such that

$$\frac{1}{2\pi}\sum_{j=1}^{N}\int_{S_B}\sigma\nabla(1\mathrm{n}\,r)dS\,.\,n$$
$$-\frac{1}{2\pi}\sum_{j=1}^{N}\int_{S_B}\mu\nabla\left[\frac{\partial}{\partial n}(1\mathrm{n}\,r)\right]dS\,.\,n$$
$$-\frac{1}{2\pi}\sum_{j=1}^{N}\int_{S_W}\mu\nabla\left[\frac{\partial}{\partial n}(1\mathrm{n}\,r)\right]dS\,.\,n+\nabla\Phi_\infty\,.\,n=0 \tag{11}$$

3.1 LOWER ORDER PANEL METHOD

An even simpler lower order panel method (constant strength source method) can be derived by setting the doublet strength μ to zero in Equation (11). Thus

$$\frac{1}{2\pi}\sum_{j=1}^{N}\int_{S_B}\sigma\nabla(1\mathrm{n}\,r)dS\,.\,n+\nabla\Phi_\infty\,.\,n=0 \tag{12}$$

Now the above equation can be written as

$$\sum_{\substack{j=1\\i=1}}^{N}a_{ij}\sigma_j+\sum_{i=1}^{N}\nabla\Phi_\infty\,.\,n=0 \tag{13}$$

where,

$$\frac{1}{2\pi}\int\nabla(1\mathrm{n}\,r)dS\,.\,n_i=(u,\,w)_{ij}\,.\,n_i=a_{ij} \tag{14}$$

The influence co-efficient a_{ij} is defined as the velocity component normal to the surface. The velocity induced by the panel $(u,\,w)_{ij}$ will be calculated by using Equations (A10) and (A11) of Appendix. Writing the term Φ_∞ in terms of velocity component, Equation (13) can be written as

$$\sum_{\substack{j=1\\i=1}}^{N}a_{ij}\sigma_j+\Sigma(U_\infty,\,W_\infty)\,.\,n_i=0 \tag{15}$$

where $(U_\infty,\,W_\infty)=-Q_\infty\,(cos\,\alpha,\,sin\,\alpha)$ and $n_i=(\sin\alpha_i,\cos\alpha_i)$. For the case of symmetric hydrofoil $W_\infty=0$ and the free stream normal velocity component is transferred to the right hand side and the following equation can be written as:

$$RHS_i=-U_\infty\,sin\,\alpha_i \tag{16}$$

At each collocation point the influences of the singularity elements (a_{ij}) are calculated and then specifying the boundary condition for each $(i=1\rightarrow N)$of the collocation points results in a set of algebraic equations with the unknown σj $(j=1\rightarrow N)$. A combination of Equations (15) and (16) will have the form

$$\begin{pmatrix}a_{11}&a_{12}&\cdot&\cdot&\cdot&\cdot&a_{1N}&\sigma_1\\a_{21}&a_{22}&\cdot&\cdot&\cdot&\cdot&a_{2N}&\sigma_2\\a_{31}&a_{32}&\cdot&\cdot&\cdot&\cdot&a_{3N}&\sigma_3\\\cdot&\cdot&\cdot&\cdot&\cdot&\cdot&\cdot&\cdot\\\cdot&\cdot&\cdot&\cdot&\cdot&\cdot&\cdot&\cdot\\\cdot&\cdot&\cdot&\cdot&\cdot&\cdot&\cdot&\cdot\\\cdot&\cdot&\cdot&\cdot&\cdot&\cdot&\cdot&\cdot\\a_{N1}&a_{N2}&\cdot&\cdot&\cdot&\cdot&a_{NN}&\sigma_N\end{pmatrix}=\begin{pmatrix}RHS_1\\RHS_2\\RHS_3\\\cdot\\\cdot\\\cdot\\\cdot\\RHS_N\end{pmatrix} \tag{17}$$

The above set of algebraic equations has a well-defined diagonal and can be solved for σ_j by using Gaussian elimination method.

3.1.1. Calculations of Pressures and Loads

Once the strengths of the sources σ_j is known, the total tangential velocity Q_t at each collocation point can be calculated as

$$Q_{ti}=\left[\sum_{\substack{j=1\\i=1}}^{N}(u,\,w)_{ij}+(U_\infty,W_\infty)\right].\,t_i \tag{18}$$

where, $t_i=(cos\,\alpha_i,\,-sin\,\alpha_i)$. Now the pressure coefficient then becomes

$$C_p=1-\frac{Q^2{}_t}{Q^2_\infty} \tag{19}$$

Note that this method is derived here for non-lifting shapes and the Kutta condition is not used. Consequently, the circulation of the hydrofoil will be zero and hence no lift and drag will be produced.

3.2 HIGHER ORDER PANEL METHOD

The formulation for the higher order panel method (linear strength source method) can be derived by setting the doublet strength μ to zero in Equation (11)

$$\frac{1}{2\pi}\sum_{j=1}^{N}\int\sigma\nabla(1\mathrm{n}\ r)dS.\ n+\nabla\Phi_{\infty}\ .\ n=0 \tag{20}$$

Now the above equation can be written as

$$\sum_{\substack{j=1\\i=1}}^{N} a_{ij}\sigma_j+\sum_{j=1}^{N}\nabla\Phi_{\infty}\ .\ n_i=0 \tag{21}$$

where,

$$\frac{1}{2\pi}\int\nabla(1\mathrm{n}\ r)dS\ .\ n_i=a_{ij} \tag{22}$$

The source-only based method will be applicable only to non-lifting configurations and is considered to be a more refined model than the one based on constant-strength source elements. The influence co-efficient a_{ij} will be calculated as follows:

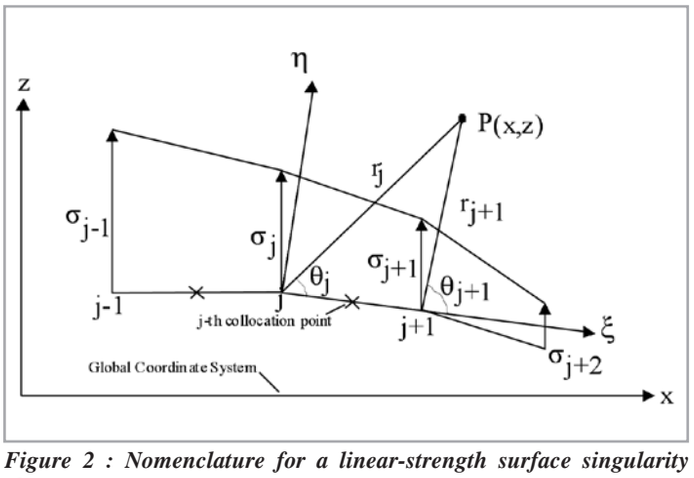

Figure 2 : Nomenclature for a linear-strength surface singularity element

A segment of the discretised singularity distribution on a solid surface is shown in Figure 2. To establish a normal-velocity boundary condition based method, the induced-velocity formulas of a constant and a linear-strength source distribution are combined by Equations (A7), (A20), (A8) and (A21) of Appendix. The parameters r and θ are shown in Figure 2 and the velocity (u, w) measured in the panel local coordinate system $p(\xi, \eta)$ has components

$$u_p=\frac{\sigma_0}{4\pi}1\mathrm{n}\frac{r_1^2}{r_2^2}+\frac{\sigma_1}{2\pi}\left[\frac{x-\xi_1}{2}1\mathrm{n}\frac{r_1^2}{r_2^2}+(\xi_1-\xi_2)+z(\theta_2-\theta_1)\right]=\left[\frac{\sigma_0}{2\pi}+\frac{\sigma_1}{2\pi}(x-\xi_1)\right]1\mathrm{n}\frac{r_1}{r_2}+\frac{\sigma_1}{2\pi}[(\xi_1-\xi_2)+z(\theta_2-\theta_1)] \tag{23}$$

$$W_p=\frac{\sigma_0}{2\pi}(\theta_2-\theta_1)+\frac{\sigma_1}{4\pi}\left[z\ 1\mathrm{n}\frac{r_2^2}{r_1^2}+2(x-\xi_1)(\theta_2-\theta_1)\right]=\frac{\sigma_1}{2\pi}z\ 1\mathrm{n}\frac{r_2}{r_1}+\frac{\sigma_0}{2\pi}(\theta_2-\theta_1)+\frac{\sigma_1}{2\pi}(x-\xi_1)(\theta_2-\theta_1) \tag{24}$$

where the subscripts 1 and 2 refer to the panel edges j and j+1 respectively. In these Equations σ_0 and σ_1 are the source strength values, as shown in Figure 3. If the strength of σ at the beginning of each panel is set equal to the strength of the source at the end point of the previous panel (as shown in Figure 2), a continuous source distribution is obtained.

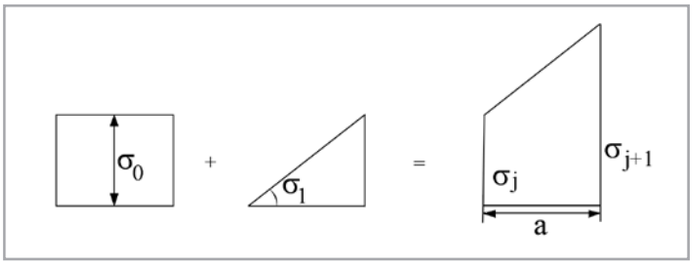

Figure 3 : Decomposition of a generic linear-strength singularity element.

Now, if the unknowns are the panel edge values of the source distribution (σ_j, $\sigma_j+{}_1$, ····· as in Figure 2) then for N surface panels on a closed body the number of unknowns is N+1. The relation between the source strengths of the elements shown in Figure 3 and the panel edge values is

$$\sigma_j=\sigma_0 \tag{25a}$$

$$\sigma_{j+1}=\sigma_0+\sigma_1 a \tag{25b}$$

where a is the panel length, and for convenience the induced-velocity equations are rearranged in terms of the panel-edge surface strengths σ_j and σ_{j+1} (and the subscripts 1 and 2 are replaced with the j and j+1 subscripts respectively):

$$u_p=\frac{\sigma_j(\xi_{j+1}-\xi_j)+(\sigma_{j+1}-\sigma_j)(x-\xi_j)}{2\pi(\xi_{j+1}-\xi_j)}1\mathrm{n}\frac{r_j}{r_{j+1}}-\frac{z}{2\pi}\frac{(\sigma_{j+1}-\sigma_j)}{(\xi_{j+1}-\xi_j)}\frac{(\xi_{j+1}-\xi_j)}{z}+(\theta_{j+1}-\theta_j) \tag{26}$$

$$w_p=\frac{z}{2\pi}\frac{(\sigma_{j+1}-\sigma_j)}{(\xi_{j+1}-\xi_j)}1\mathrm{n}\frac{r_{j+1}}{r_j}+\frac{\sigma_j(\xi_{j+1}-\xi_j)+(\sigma_{j+1}-\sigma_j)(x-\xi_j)}{2\pi(\xi_{j+1}-\xi_j)}+(\theta_{j+1}-\theta_j) \tag{27}$$

Note that Equations (26) and (27) can be divided into velocity induced by σ_j and by σ_{j+1} such that

$$(u,\ w)_p=(u^a,\ w^a)_p+(u^b,\ w^b)_p \tag{28}$$

where the subscript $(\ )^a$ and $(\ )^b$ represent the contribution due to the leading and trailing singularity strengths, respectively. If Equations (26) and (27) are arranged we can separate the $(\ )^a$ part of the velocity components as,

$$u_p^a=\frac{\sigma_j(\xi_{j+1}-x)}{2\pi(\xi_{j+1}-\xi_j)}1\mathrm{n}\frac{r_j}{r_{j+1}}+\frac{z}{2\pi}\left(\frac{\sigma_j}{\xi_{j+1}-\xi_j}\right)\left[\frac{(\xi_{j+1}-\xi_j)}{z}+(\theta_{j+1}-\theta_j)\right] \tag{29a}$$

$$w_p^a = \frac{z}{2\pi}\left(\frac{\sigma_j}{(\xi_{j+1}-\xi_j)}\right) \ln\frac{r_{j+1}}{r_j} + \frac{\sigma_j(\xi_{j+1}-x)}{2\pi(\xi_{j+1}-\xi_j)}(\theta_{j+1}-\theta_j) \quad (29b)$$

from the $(\ )^b$ part of the velocity components,

$$u_p^b = \frac{\sigma_{j+1}(x-\xi_j)}{2\pi(\xi_{j+1}-\xi_j)} \ln\frac{r_j}{r_{j+1}} - \frac{z}{2\pi}\left(\frac{\sigma_{j+1}}{\xi_{j+1}-\xi_j}\right)\left[\frac{(\xi_{j+1}-\xi_j)}{z} + (\theta_{j+1}-\theta_j)\right] \quad (29c)$$

$$w_p^b = -\frac{z}{2\pi}\left(\frac{\sigma_{j+1}}{\xi_{j+1}-\xi_j}\right) \ln\frac{r_{j+1}}{r_j} + \frac{\sigma_{j+1}(x-\xi_j)}{2\pi(\xi_{j+1}-\xi_j)}(\theta_{j+1}-\theta_j) \quad (29d)$$

To transform these velocity components back to the (x, z) coordinates, a rotation by the panel orientation angle α_i is performed by the following equation:

$$\begin{bmatrix} u \\ w \end{bmatrix} = \begin{bmatrix} \cos\alpha_i & \sin\alpha_i \\ -\sin\alpha_i & \cos\alpha_i \end{bmatrix} \begin{bmatrix} u \\ w \end{bmatrix}_p \quad (30)$$

The velocity at each collocation point is influenced by the two edges of the j-th panel. Thus, adding the influence of the (j+1)-th panel and each subsequent panel gives the local induced velocity at the first collocation point

$$\begin{aligned}(u, w)_1 &= (u^a, w^a)_{11}\sigma_1 + [(u^b, w^b)_{11} + (u^a, w^a)_{12}]\sigma_2 \\ &+ [(u^b, w^b)_{12} + [(u^a, w^a)_{13}]\ \sigma_3 + \ldots\ldots\ldots \\ &= [(u^b, w^b)_{1,N-1} + [(u^a, w^a)_{1N}]\sigma_N + (u^b, w^b)_{1N}\sigma_{N+1}\end{aligned}$$

This equation can be reduced to a form

$$(u, w)_1 = (u, w)_{11}\sigma_1 + (u, w)_{12}\sigma_2 + \ldots\ldots + (u, w)_{1N+1}\sigma_{N+1}$$

such that for the first and last terms

$$(u, w)_{11} = (u^a, w^a)_{11} \quad (31a)$$

$$(u, w)_{1,N+1} = (u^b, w^b)_{1N}\sigma_{N+1} \quad (31b)$$

and for all other terms

$$(u, w)_{1,j} = [(u^b, w^b)_{1,j-1} + (u^a, w^a)_{1,j}]\ \sigma_j \quad (31c)$$

From this point the procedure is similar to the constant-strength source method. The influence coefficient is calculated when $\sigma_j = 1$ and

$$a_{ij} = (u, w)_{ij} \cdot n_i \quad (32)$$

For each collocation point there will be N+1 such coefficients and unknowns σ_j. The free-stream normal velocity components RHS_i is found at the collocation point

$$RHS_i = -U_\infty \sin\alpha_i \quad (33)$$

where α_i is the panel inclination angle. Specification of the boundary condition for each ($i = 1 \rightarrow N$) of the collocation points result in N linear algebraic equations with the unknowns σj ($j = 1 \rightarrow N$+1). The additional equation can be found by requiring that the flow leaves parallel to the trailing edge: thus

$$\sigma_1 + \sigma_{N+1} = 0 \quad (34)$$

Another option that will yield similar results is to establish an additional collocation point slightly behind the trailing edge and require that the velocity will be zero there (stagnation point for finite-angle trailing edges). A combination of Equation (21), (33) and (34) with the N boundary conditions result in following (N+1) linear equations:

$$\begin{pmatrix} a_{11} & a_{12} & \cdots & a_{1.N+1} \\ a_{21} & a_{22} & \cdots & a_{2.N+1} \\ a_{31} & a_{32} & \cdots & a_{3.N+1} \\ \vdots & \vdots & \cdots & \vdots \\ a_{N1} & a_{N2} & \cdots & a_{N.N+1} \\ 1 & 0 & \cdots & 1 \end{pmatrix} \begin{pmatrix} \sigma_1 \\ \sigma_2 \\ \sigma_3 \\ \vdots \\ \sigma_N \\ \sigma_{N+1} \end{pmatrix} = \begin{pmatrix} RHS_1 \\ RHS_2 \\ RHS_3 \\ \vdots \\ RHS_N \\ 0 \end{pmatrix} \quad (35)$$

The above set of algebraic equations has a well-defined diagonal and can be solved for σ_j by using standard methods of linear algebra.

3.2.1. Calculation of Pressures and Loads

Once the strength of the sources σ_j is known, the velocity at each collocation point can be calculated and the pressure coefficient can be calculated by using Equation (19).

4.0 RESULTS AND DISCUSSIONS

The numerical algorithms outlined before have been applied to a number of hydrofoils such as van de Vooren and NACA 0012 in order to analyse the hydrodynamic characteristics at various depths of water. In the first case, source based lower order panel method with Neumann boundary condition is applied to the 15% thick symmetric van de Vooren hydrofoil with an angle of attack, $\alpha = 0°$. The hydrofoil is discretised by $M = 90$ panels. The predicted pressure on van de Vooren hydrofoil is compared with its analytical results in Figure 4 and the agreement is quite satisfactory. The pressures on this hydrofoil at various depths of water such as respectively are plotted in Figure 5 and we can see that the effect of the depths of water is insignificant. Discretising the hydrofoil by 40, 90 and 180 panels respectively, source based lower order panel method has also been applied to van de Vooren hydrofoil at a depth of water $h/c = 0.4$. Note that this method is derived here for nonlifting shapes and the Kutta condition is not used. Consequently, the circulation of the hydrofoil will be zero and hence no lift and drag will be produced. However, the pressure distribution is well predicted in *Figure 6* and they are convergent to one another. The numerical solution presented here does not assume a symmetric solution. But it appears that the solution is symmetric about the x-axis and the number of unknowns can be reduced by M/2 by a minor modification in the process of influence co-efficient.

A comparison of pressure distribution on van de Vooren hydrofoil with an angle of attack, $\alpha = 0°$ calculated from source based higher order panel method is drawn in Figure 7. It is noted that each computational method depends on the grid and on various other parameters. Therefore, each technique must be validated first before it can be applied to unknown cases. The sensitivity of the linear higher order panel method with Neumann boundary condition is presented in Figure 8. Both methods will have problems near the trailing edge. The calculated values of C_p on NACA 0012 hydrofoil are also compared with Fletcher's numerical as well as Amick's experimental results (Fletcher, 1991) in Figure 9. The agreement between the experimental

result and that of lower order method is better in compared to higher order method. Higher order method can achieve a prescribed level of accuracy but the code is more complicated and the required amount of computation per panel is higher. However, the relative merits of low and high order methods depend on the specific problem and on the fundamental method being used.

The computation times measured in seconds (of Intel Celeron computer, 2.00 GHZ and 248 MB of RAM) versus the number of panels is presented in Figure 10. These data indicate that the lower order panel method is the faster and computational effort increases with increasing the order of the method.

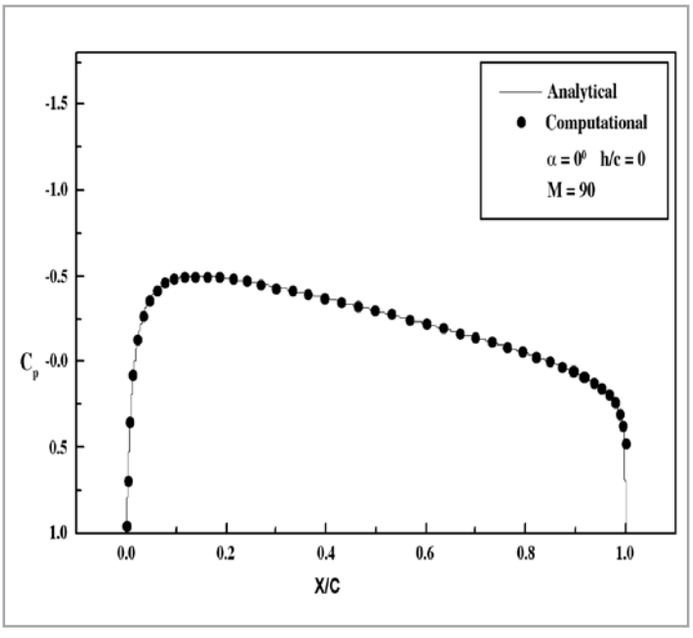

Figure 4 : Pressure on van de Vooren hydrofoil at h/c = 0 by the lower order panel method

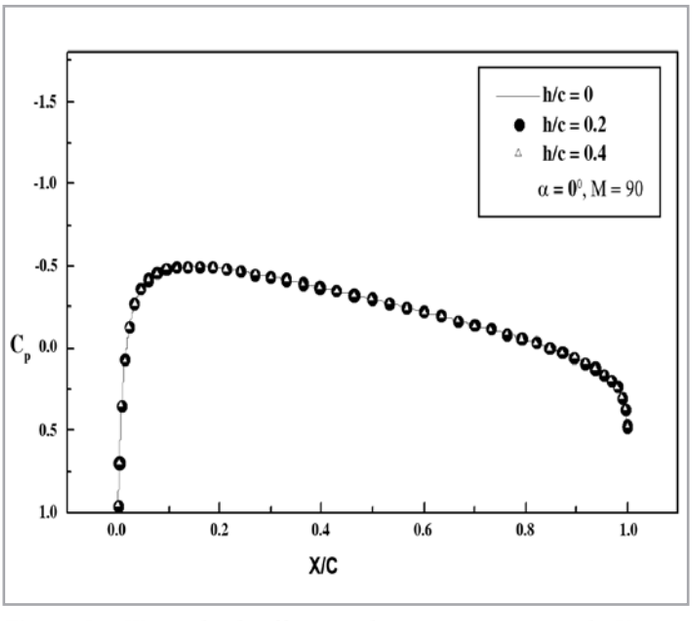

Figure 5 : Water depth effect on the pressure on van de Vooren hydrofoil by the lower order panel method

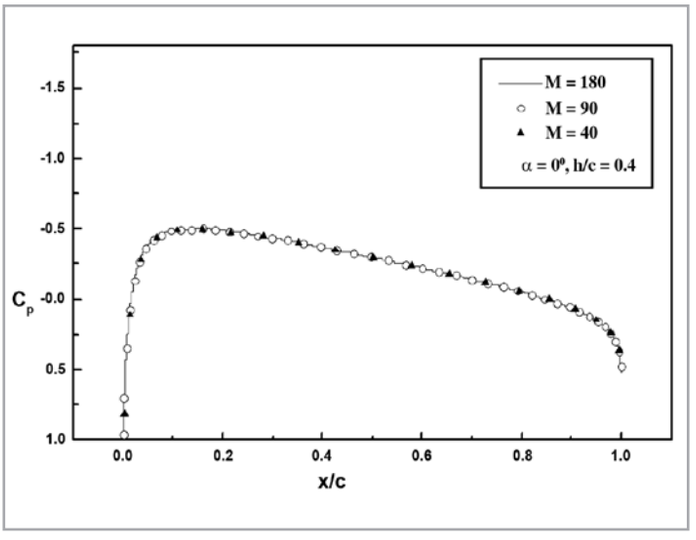

Figure 6 : Panel size effect on the pressure on van de Vooren hydrofoil at h/c = 0.4 by the lower order panel method

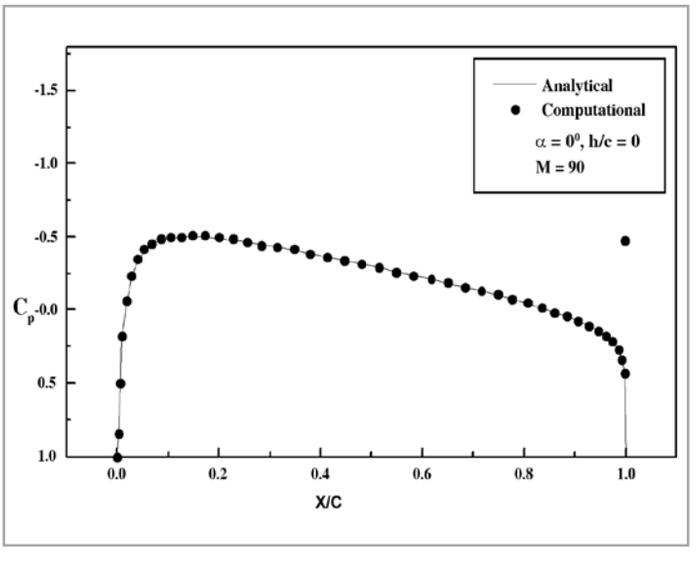

Figure 7 : Pressure on van de Vooren hydrofoil at h/c = 0 by the higher order panel method

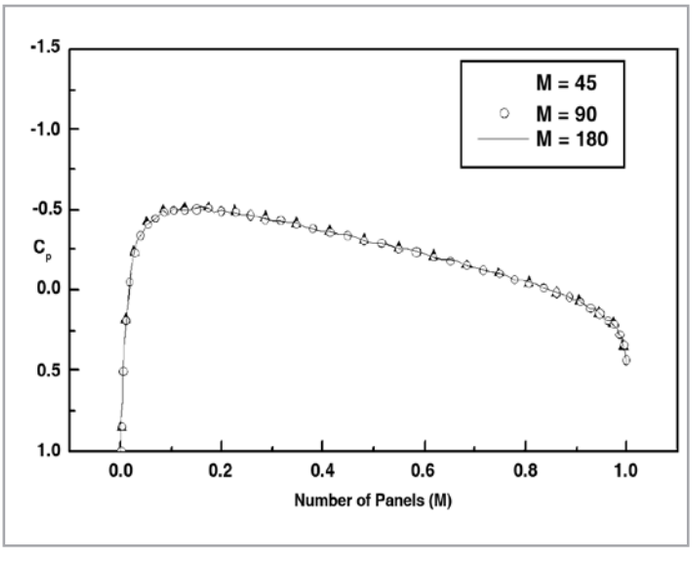

Figure 8 : Panel size effect on the pressure on van de Vooren hydrofoil at h/c = 0 by the higher order panel method

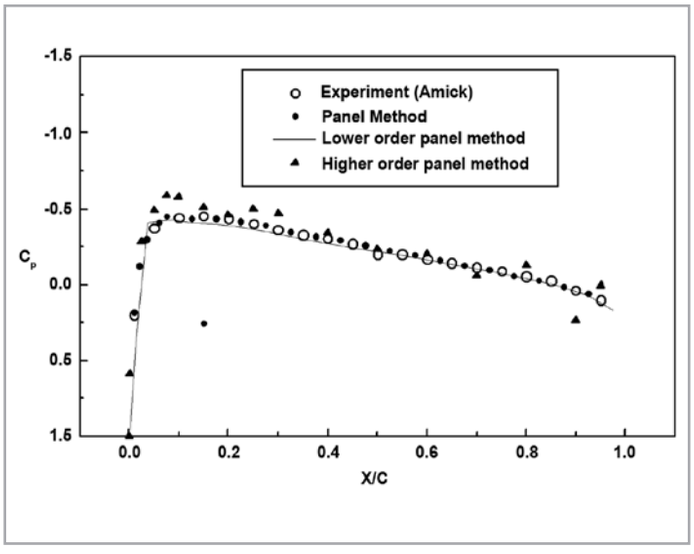

Figure 9 : Comparison between calculated and experimental Pressures on NACA 0012 hydrofoils at h/c = 0

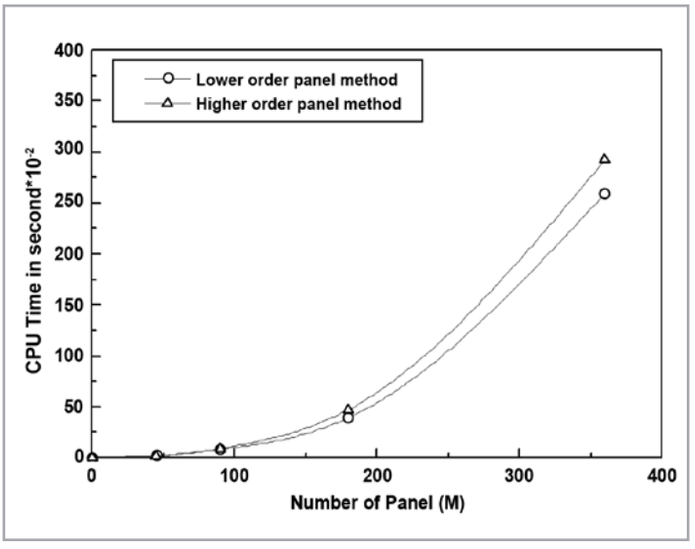

Figure 10 : Comparison of CPU time for Lower and higher order panel methods

5.0 CONCLUSIONS

The paper deals with the source based lower and higher order panel methods for computing the potential flow around the hydrofoil moving with a uniform speed in an unbounded fluid. The following conclusions can be drawn from the present study:

(i) In general, the use of the lower order method results in fewer numerical manipulations and hence less computational time. The use of higher order method requires more computational effort and is justified when the velocity near the body is continuous.

(ii) Each computational method depends on the grid and on various other parameters. Therefore, each technique must be validated before it is applied to unknown cases.

(iii) Both the methods have the problems near the cusped trailing edge of the hydrofoil. Such problems may be avoided by modeling a finite angle there (instead of zero angle) and this may be achieved by simply having larger trailing-edge panels.

(iv) The agreement between the present numerical results with the analytical as well as experimental results is quite satisfactory. ■

APPENDIX

INFLUENCE CO-EFFICIENT

Lower Order Panel Method

Consider a source distribution along the ξ axis as shown in Figure 11. It is assumed that the source strength per unit length is constant such that σ (ξ) = σ = const. The influence of this distribution at a point *P* (*x, z*) is an integral of the influences of the point elements along the segment $\xi_1 - \xi_2$ (see Islam, 2008):

$$\Phi = \frac{\sigma}{2\pi} \int_{\xi_1}^{\xi_2} 1n \sqrt{(x-\xi)^2 + z^2}\, d\xi \qquad \text{(A1)}$$

Differentiating Equation (A1) with respect to *x* and *z*

$$u(\xi, \eta) = \frac{\sigma}{2\pi} \int_{\xi_1}^{\xi_2} \frac{x-\xi}{(x-\xi)^2 + z^2}\, d\xi \qquad \text{(A2)}$$

$$w(\xi, \eta) = \frac{\sigma}{2\pi} \int_{\xi_1}^{\xi_2} \frac{z}{(x-\xi)^2 + z^2}\, d\xi \qquad \text{(A3)}$$

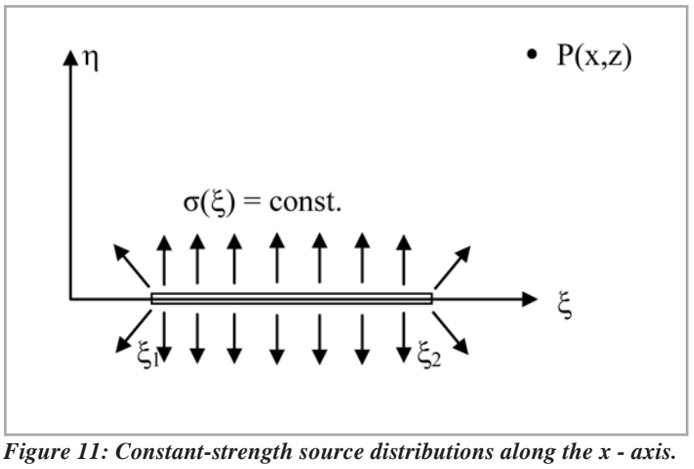

Figure 11: Constant-strength source distributions along the x - axis.

The integral for the velocity potential in terms of the corner points (ξ_1, 0) and (ξ_2, 0) of a generic panel element as shown in Figure 12, the distances r_1, r_2 and the angles θ_1, θ_2 it becomes

$$\Phi = \frac{\sigma}{4\pi} [(x-\xi_1)\ 1n\ r^2_1 - (x-\xi_2)\ 1n\ r^2_2 + 2z(\theta_2 - \theta_1)] \qquad \text{(A4)}$$

where

$$\theta_k = tan^{-1} \frac{z}{x-\xi_k} \qquad k = 1, 2 \qquad \text{(A5)}$$

$$r_k = \sqrt{(x - \xi_k)^2 + z^2} \qquad k = 1, 2 \qquad \text{(A6)}$$

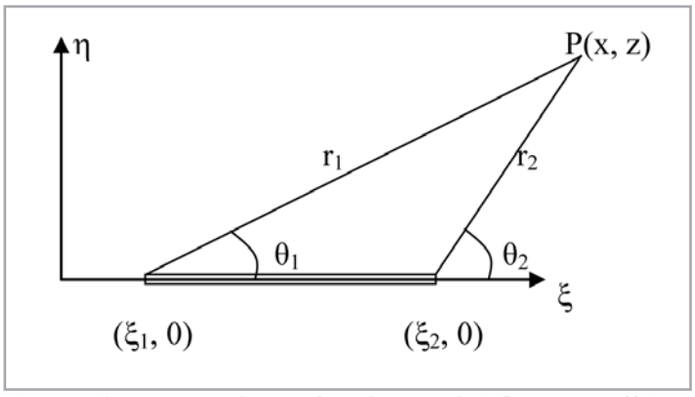

Figure 12 : Nomenclature for the panel influence coefficient derivation

The velocity components are obtained from Equation (A2) and (A3) as

$$u = \frac{\sigma}{2\pi} \ln \frac{r_1}{r_2} = \frac{\sigma}{4\pi} \ln \frac{r_1^2}{r_2^2} \qquad \text{(A7)}$$

$$w = \frac{\sigma}{2\pi} (\theta_2 - \theta_1) \qquad \text{(A8)}$$

Returning to *x, z* variables we obtain

$$\Phi = \frac{\sigma}{4\pi} \{(x - \xi_1) \ln[(x - \xi_1)^2 + z^2] - (x - \xi_2) \ln[(x - \xi_2)^2 + z^2 + 2z (tan^{-1} \frac{z}{x - \xi_2} - tan^{-1} \frac{z}{x - \xi_1})\} \qquad \text{(A9)}$$

$$u = \frac{\sigma}{4\pi} \ln \frac{(x - \xi_1)^2 + z^2}{(x - \xi_2) + z^2} \qquad \text{(A10)}$$

$$w = \frac{\sigma}{2\pi} \left[tan^{-1} \frac{z}{x - \xi_2} - tan^{-1} \frac{z}{x - \xi_1} \right] \qquad \text{(A11)}$$

HIGHER ORDER PANEL METHOD

Let us consider a linear source distribution along the ξ axis ($\xi_1 < \xi < \xi_2$) with a source strength of $\sigma(\xi) = \sigma_0 + \sigma_1(\xi - \xi_1)$, as shown in Figure 13. Based on the principle of superposition, this can be divided into a constant-strength element and a linearly varying strength element with the strength $\sigma(\xi) = \sigma_1 \xi$. Therefore, for the general case as shown in the left-hand side of Figure 13, the results of this section must be added to the results of the constant-strength source element.

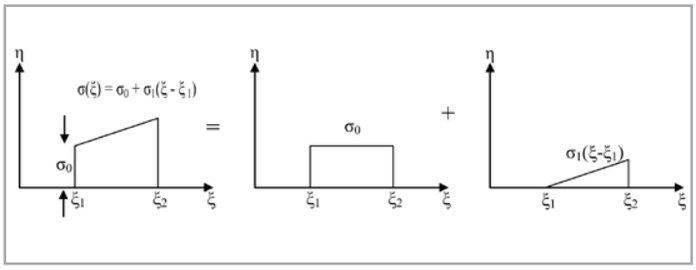

Figure 13 : Decomposition of a generic linear strength element to constant-strength and linearly varying strength elements

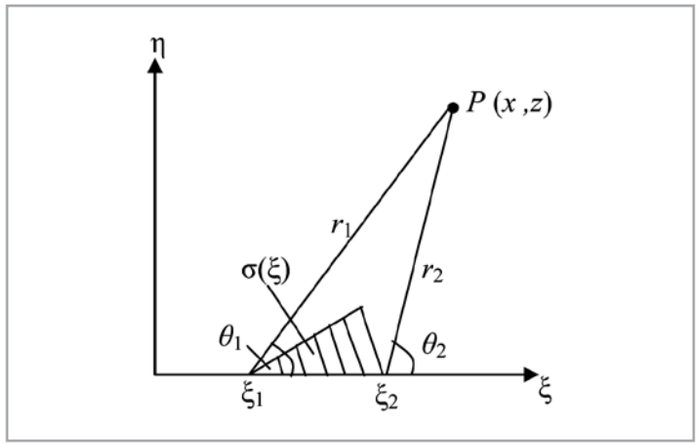

Figure 14 : Nomenclature for calculating the influence of linearly varying strength source

The influence of the simplified linear distribution source element, where $\sigma(\xi) = \sigma_1 \xi$, at a point *P* is obtained by integrating the influences of the point elements between ξ_1 and ξ_2 (see Figure 14):

$$\Phi = \frac{\sigma_1}{2\pi} \int_{\xi_1}^{\xi_2} \xi \ln \sqrt{(x - \xi)^2 + z^2}\, d\xi \qquad \text{(A12)}$$

$$u = \frac{\sigma_1}{2\pi} \int_{\xi_1}^{\xi_2} \frac{\xi(x - \xi)}{(x - \xi)^2 + z^2}\, d\xi \qquad \text{(A13)}$$

$$w = \frac{\sigma_1}{2\pi} \int_{\xi_1}^{\xi_2} \frac{\xi z}{(x - \xi)^2 + z^2}\, d\xi \qquad \text{(A14)}$$

The integration of the velocity potential can be represented as

$$\Phi = \frac{\sigma_1}{2\pi} \left[\frac{x^2 - \xi_1^2 - z^2}{2} \ln r_1^2 - \frac{x^2 - \xi_2^2 - z^2}{2} \ln r_2^2 + 2xz(\theta_2 - \theta_1) - x(\xi_2 - \xi_1) \right] \qquad \text{(A15)}$$

where r_1, r_2, θ_1 and θ_2 are defined by Equations (A5) and (A6). The velocity components are obtained by Equations (A13) and (A14) as follows:

$$u = \frac{\sigma_1}{2\pi} \left[\frac{x}{2} \ln \frac{r_2^2}{r_1^2} + (\xi_1 - \xi_2) + z(\theta_2 - \theta_1) \right] \qquad \text{(A16)}$$

$$w = \frac{\sigma_1}{2\pi} \left[z \ln \frac{r_2^2}{r_1^2} + 2x(\theta_2 - \theta_1) \right] \qquad \text{(A17)}$$

Substitution of r_k and θ_k from Equations (A6) and (A7) results in

$$\Phi = \frac{\sigma_1}{4\pi} \left[\frac{x^2 - \xi_1^2 - z^2}{2} \ln [(x - \xi_1)^2 + z^2] - \frac{x^2 - \xi_2^2 - z^2}{2} \ln [(x - \xi_2)^2 + z^2] + 2xz(tan^{-1} \frac{z}{x - \xi_2} - tan^{-1} \frac{z}{x - \xi_1}) - x(\xi_2 - \xi_1) \right] \qquad \text{(A18)}$$

$$u = \frac{\sigma_1}{2\pi}\left[\frac{x}{2}\,1n\,\frac{(x-\xi_1)^2+z^2}{(x-\xi_2)^2+z^2} + (\xi_1-\xi_2) + z\left(tan^{-1}\frac{z}{x-\xi_2} - tan^{-1}\frac{z}{x-\xi_1}\right)\right] \quad \text{(A19)}$$

$$w = \frac{\sigma_1}{4\pi}\left[z\,1n\,\frac{(x-\xi_1)^2+z^2}{(x-\xi_2)^2+z^2} + 2x\left(tan^{-1}\frac{z}{x-\xi_2} - tan^{-1}\frac{z}{x-\xi_1}\right)\right] \quad \text{(A20)}$$

REFERENCES

[1] Giesing, J.P. and Smith, A.M.O. (1967): Potential flow about two-dimensional hydrofoils, Journal of Fluid Mechanics, Vol. 28, pp.113-129.

[2] Hough, G.R. and Moran, S.P. (1969): Froude number effects on two-dimensional hydrofoils, Journal of Ship Research, Vol.13, pp.53-60.

[3] Salvesen and Von Kerczek, C. (1975): Numerical solution of two-dimensional nonlinear body-wave problems. Proceedings, 1st International Conference on Numerical Ship Hydrodynamics, Bethesda, pp. 279-293.

[4] Salvesen and Von Kerczek, C. (1976): Comparison of numerical and perturbation solution of two-dimensional nonlinear water-wave problems, Journal of Ship Research, Vol. 20(3), pp.160-170.

[5] Bai, K.J. (1978): A localized finite-element method for two-dimensional steady potential flows with a free surface, Journal of Ship Research, Vol. 22, pp.216-230.

[6] Yeung, R.W. and Bouger, Y.C. (1979): A hybrid-integral equation method for steady two-dimensional ship waves, International Journal of Numerical Methods in Engineering, Vol.14, pp.317-336.

[7] Kennell, C. and Plotkin, A. (1984): A second order theory for the potential flow about thin hydrofoils, Journal of Ship Research, Vol. 28, pp.55-64.

[8] Forbes, L.K. (1985): A numerical method for non-linear flow about a submerged hydrofoil, Journal of Engineering Mathematics, Vo.19, pp.329-339.

[9] Bai, K.J. and Han, J.H. (1994): A localized finite element method for the nonlinear steady waves due to a two-dimensional hydrofoil, Journal of Ship Research, Vol.38, pp.42-51.

[10] Wu, G.K. and Eatock Taylor, R. (1995): Time stepping solutions of the two dimensional nonlinear wave radiation problem, International Journal of Ocean Engineering, Vol.22, pp.785-798.

[11] Bal, S. (1999): A panel method for the potential flow around 2-D hydrofoil, Transactions of Journal of Engineering and Environmental Science, Vol. 23, pp.349-361.

[12] Bal, S. (2005): Lift and drag characteristics of cavitating swept and V-type hydrofoils, International Journal of Maritime Engineering, The Royal Institute of Naval Architects.

[13] Tarafder, M. S., Khalil, G. M. and Mahmud, S. M. I. (2006): Free surface potential flow around Hydrofoils by Rankine source panel method, The Journal of National Oceanographic and Maritime Institute, Vol. 23, No. 2, pp.57-75.

[14] Hsin, C.Y. and Chou, S.K. (1998): Applications of a hybrid boundary element method to the analysis of free surface flow around lifting and non-lifting bodies, Proceedings of the 22nd Sympossium on Naval Hydrodynamics, Washington DC, USA.

[15] Kim, B.K. (1992): Computation of hydrodynamic forces on a submerged lifting body, Proceedings of the 2nd International Offshore and Polar Engineering Conference, ISOPE, San Francisco, USA, June 14-19, pp 367-374.

[16] Ragab, S.A. (1998): Inviscid non-cavitating flow over shallowly submerged swept hydrofoils, Proceedings of the 8th International Offshore and Polar Engineering Conference, ISOPE, Montreal, Canada, May 24-29, pp. 253-259.

PROFILES

DR MD SHAHJADA TARAFDER

Dr Md. Shahjada Tarafder is now working as an Associate Professor in the Department of Naval Architecture and Marine Engineering of Bangladesh University of Engineering and Technology, Dhaka. Dr Tarafder obtained the Degree of B Sc Engg. in 1994 and M Sc Engg. in 1996 from the same university. He obtained the Degree of Doctor of Engineering from Yokohama National University, Japan in September 2002.

DR GAZI M KHALIL

Dr Gazi M. Khalil is serving as a Professor in the Department of Naval Architecture and Marine Engineering of Bangladesh University of Engineering and Technology, Bangladesh. He has been teaching and doing research in this university for more than 35 years. Dr Khalil has to his credit more than 100 research papers published in various national and international journals and proceedings of the conferences. He has been serving as the Editor of the Journal of NOAMI published by the National Oceanographic and Maritime Institute, Bangladesh since 1997 to till to-date.

MR. MUHAMMAD RABIUL ISLAM

Mr. Muhammad Rabiul Islam is an Assistant Naval Architect of Bangladesh Inland Water Transport Authority (BIWTA), Ministry of Shipping of Bangladesh. Currently, he is doing his Ph D in Yokohama National University, Japan. He received the Degree of M Sc Engg. in 2008 and B Sc Engg. in 2003 from the Department of Naval Architecture and Marine Engineering of Bangladesh University of Engineering & Technology, Dhaka.